Santomaso, A.C., Lazzaro P., Canu, P. Powder flowability and density ratios: the impact of granule packing (2003) *Chemical Engineering Science,* 58 (13), pp. 2857-2874.
DOI:10.1016/S0009-2509(03)00137-4

Powder Flowability and Density Ratios: the Impact of Granules Packing

A. Santomaso, P. Lazzaro, P. Canu*
Università di Padova, Dipartimento di Principi e Impianti di Ingegneria Chimica,
Via Marzolo 9, 35131 Padova, Italy

Keywords: Powders, Flowability, Granular, Packing, Apparent density, Imaging

Abstract

The propensity of powders to flow under given circumstances (flowability) affects a large number of industrial applications. A single, reliable and widely applicable flowability test does not exist, because of the variety of both granular materials and influence of handling on the measurements results. Here we critically examined the results provided by Hausner's method, based on apparent densities ratio, with several granular materials. Major limitations appeared to be the achievement and measurement of a dense packing condition, provided by the tapped density in the Hausner's ratio. After a detailed discussion of standard and modified techniques to measure bulk density, we eventually suggest a new flowability criterion based on a novel technique to determine a high packing density. The proposed criterion is more sensitive to differences in flowability, as quantified by the repose angle. In order to investigate also the domain of cohesive powders, we developed a novel procedure to measure the repose angle of such powders. Eventually, the new criterion was able to account consistently for free-flowing and cohesive powders. It also stimulates the discussion on subtle issues involved in the determination and use of elementary powder's properties.

1. Introduction

The impact of granular material on the chemical industry has been frequently recalled. Design, operation and quality assurance in many industrial processes involving granular material heavily rely on the ability to quantitatively determine the propensity of powders to flow, usually called flowability. Cases include silos discharge, transport operation, mixing, valves for solids dosage (L-, J-, V-valves), fluidization, and many others. Free flowing powders are usually sought because they are easier to handle and hence do not frequently cause difficulties on the plants. However, free flowing powders are known to easily segregate by size when used with a polidispersed particles size distribution (PSD). The opposite is the case of cohesive or poorly flowing powders (Bates, 1996). Consequently, being able to determine the flowing properties of a granular material is crucial to prevent serious problems during production processes.

There are many techniques to determine the flowability of powders aiming to describe the state of the powder in the process under consideration (De Jong *et al.*, 1999). They can be classified between methods that directly observe the behavior of the granular material during flow in its consolidated state (direct methods) and those that determine flow properties expected to be connected with the flowability in its loosely packed state (indirect methods). Among the first ones we mention shear cells, like Jenike cell, annular cells, triaxial cells, and true biaxial testers (Schwedes, 1996). Indirect methods refer to static and dynamic angle of repose, discharge time under given circumstances

* Corresponding author. Tel.: +39 049 8275463; fax: +39 049 8275461;
E-mail: paolo.canu@unipd.it

(ASTM B 213), fluidization degree, and powder deaeration rate. Propensity to pack is another flowability index used to describe the behavior of loosely packed powders, the one we concentrate on in this work. An external force field, typically gravity, can promote a higher packing of granules, which occurs through relative particle motion. A comparison among different degrees of packing can be a measure of the difficulties experienced by the particles to rearrange their positions in the bed and hence to macroscopically flow.

Note that packing we consider to be the particles rearrangement towards a reduction of interparticle voidage without affecting the original particle shape and dimension. Packing must not be confused with compaction, which implies morphological modifications of the granules.

Packing of a granular material is usually quantified by apparent (bulk) densities, that are always defined as the ratio between the sample mass and its total volume, including any internal interstice, both inter- and intraparticle. There are different formulations based on the procedure used to achieve the desired packing (Svarovsky, 1987).

Aerated density is meant to be the lowest degree of packing under gravity. It can be determined allowing the powder to settle by gravity either from a fluidized condition or through a vibrating sieve like in the Hosokawa Powder Tester (Abdullah & Geldart, 1999).

Poured density is perhaps the most widely used so that it is frequently referred as *apparent density* without further specification. Accordingly, it is the subject of standard procedures (ISO 3923-1 or equivalently ASTM B 212, ASTM B 417, and EN 23923-1). The method prescribes filling a 25 mL cup from a hopper, 2.5 cm above it. Originally developed for metallic powders, it is normally used for any powder that flows through orifices of 2.5 and 5 mm. Variations are suggested for those cases when discharge does not occur (ISO 3923-2 and ISO 3923-3, or equivalently ASTM B 329, ASTM B 703, and EN 23923-2), including larger orifices, vibrating funnels and modified feeding devices.

Both aerated and poured density aim at achieving a condition of *loose random packing*. Alternative, non standard procedures have been suggested by Scott (1960) and Zou & Yu (1996), that use a cylindrical container, slowly rotated horizontally and then tilted in its vertical position to measure the apparent powder volume.

Tap density is obtained by vibration or hitting the collecting cup according to a given procedure, in an attempt to obtain the highest packing (and density then) before compaction. In practice it is difficult to prevent any compaction while hitting a powder. Limited to the case of metallic powders a procedure has been standardized (ISO 3953, or equivalently ASTM B 527, EN 23953). It requires vertically hitting a graduated container until the powder bed stabilizes at a minimum volume. A non-standard procedure is the Hosokawa Powder Tester (Abdullah & Geldart, 1999) already mentioned.

For non-metallic powders, such as ceramics and plastics, other standard procedures exist, based on the same goal of packing as much as possible (e.g. ASTM D 1895 for plastics or EN 725-8 for ceramics). Procedures for pharmaceutical powders are usually given by local, official pharmacopeias in terms of number of strokes required to achieve a dense packing condition (10, 500, 1250 strokes in the European Pharmacopoeia, 1993).

In the case of tap density, the condition sought is that of a *dense random packing* to be contrasted with the *loose random packing* state of the apparent density. It has been observed that the flowability is connected with the ratio of a ‘high’ to a ‘low’ density value. The ‘high’ density condition must be obtained by somehow forcing the powder to pack as much as possible (but not

compact), while the 'low' density state is that of minimum packing that the granules can maintain naturally, without continuous addition of some sort of force (such as fluidizing air). The higher the ratio between 'high' and 'low' density values, the more cohesive is the powder, or the less able to flow.
We used vague adjectives above (i.e. 'high' and 'low') because our short review of density definitions allows concluding that there are many density definitions, corresponding to different, frequently non-standard procedures to obtain them.
Moreover, established flowability indices, such as the Hausner ratio, *HR*, are not always used with the same densities, mostly because of the alternatives in the 'low' density measurement techniques. Someone (Harnby *et al.*, 1987 e Abdullah & Geldart, 1999) used *HR* as the ratio between tap and aerated density, while others (Wong, 2000) used tap and poured densities. Zou & Yu (1996) used the apparent density determined by the method of Scott (1960).

2. Density of highly packed powders

Our experimental measurements of different density values, according to several techniques, allowed us to conclude that the loose random packing can be almost uniquely determined, whatever the method used. Accordingly, the different *HR* definitions mentioned above are not expected to result in significantly different values because of the type of 'low' density involved. On the contrary, it was apparently never reported before that the dense random packing condition is much more difficult to obtain reproducibly. Tap density measurements are strongly affected by the frequency, the amplitude and the total number of strokes or vibrations impressed to the sample, the nature of which does not allow standardizing any universally valid value for these parameters. The dependence of the technique on the nature of the granular material is the most undesired feature and we dedicated this work to an effort of freeing the results of several measuring techniques from such a constraint. The degree of achievement of our goal will be detailed in the following, but we can anticipate that a critical, frequently simple revision of the procedures can result in significant advancements.
Packing modes of rigid, monodispersed spheres have been an interest of physicists since a long time, because they are considered a model for simple liquids (Scott, 1960; Bernal & Mason, 1960). Dynamics of such collection of spheres has been given some attention also recently (Knight *et al.*, 1995). They experimentally observed that apparent density variation with strokes number shows relaxation phenomena, passing through several metastable conditions. All sizes of monodispersed glass spheres tested, result in a density development obeying an equation like

$$\rho = \rho_0 - \frac{\Delta\rho}{\left[1 + B\ln\left(1 + \frac{N}{\tau}\right)\right]} \qquad (1)$$

where ρ_0, $\Delta\rho$, τ, and B are parameters depending only on the vibration intensity Γ (the ratio between maximum acceleration impressed and gravity) and N is the number of strokes. Eq. (1) describes a progressive increase of granular material density when shaken beyond a given threshold of Γ. It has been suggested that packing results from cooperative movements of particles clusters, leading to internal relaxation. A theoretical explanation effort of the parameters involved in eq. (1) is reported by Linz (1996). While the increase of packing with shaking time was qualitatively expected, more interestingly Novak *et al.*, (1997) demonstrated that the packing history, and specifically the initial arrangement of the particles can dramatically affect the maximum packing achievable. They showed

for rigid spheres that packed density higher than expected for random dense packing (volumetric solid fraction, ν, equal to 0.64) can be obtained, starting from a random loose packing (ν=0.58 in their case). This conclusion follows the observation that the density changes with the history of the vibration intensity. Their interesting results are synthetically reported in Fig. 1, which shows that the non-linear increase of density with Γ is not reversible. The local maximum density (B) can increase further by a decrease of Γ, along a different, reversible path (B-C). Afterwards, the density will be only a value comprised between B and C depending on Γ. Note that shaking intensity Γ must be high enough to overcome metastable, lower density conditions of the irreversible branch, in order to access the higher packing of the reversible branch. Edwards & Grinev (1998) provided a qualitative, theoretical explanation of this behavior, applying statistical mechanics techniques (Edwards & Oakeshott,1989).

Pouliquen *et al.* (1997) were also able to obtain solid fraction in excess of 0.64, still working with glass spheres (d_p=1.98 mm). They fed the particles through a dispersed flow in a horizontally vibrating cup. The resulting bed appeared to be regularly packed in crystalline structures, with a value of ν as high as 0.67. They also noticed that the packing process was entirely determined by the dynamics of a surface layer, extending from the free surface down to a maximum of 6 particles diameters, depending on the vibration intensity. In their particular arrangement, the feed flow rate also plays a role, preventing any regular packing when excessively large.

Still another technique to break the limit of ν=0.64 was suggested by Lesaffre *et al.* (2000). They packed smaller (0.5 mm) glass spheres through purely vertical vibrations by immersing them in silicon, newtonian oils of different viscosity. Main differences are a slower process because of buoyancy and viscosity, and higher final densities (ν=0.647) thanks to lubrication. Also in this case a logarithmic law similar to eq. (1) of Knight *et al.* (1995) can describe the results, confirming the cooperative nature of the process.

The results described above, including eq. (1), apply to ideal granular materials, namely smooth, monodispersed spheres. Addressing real particles, a number of factors must be taken into account, including size and shape distributions, surface roughness, environmental and solids humidity, electrostatic susceptibility, and perhaps others. The role of each factor has not been thoroughly investigated individually, and many factors tend to affect the experiments at the same time, resulting in mostly qualitative indications. Particle size distribution (PSD) has been given most of the attention with both theoretical and experimental contributions. Mathematical models to predict the porosity (i.e. 1-ν) have been suggested in cases of mixtures of different diameter spheres (Ouchiyama & Tanaka, 1989; Yu & Standish, 1991), for irregularly shaped particles (Tsirel, 1997), and for fine powders (Yu *et al.*, 1997). Purely experimental contributions to the case of non-ideal particles have been given by Suzuki *et al.* (2001), who studied PSD effects on tap density using fine particles (below 100 μm) of silica and fly ash, and by Zou & Yu (1996) who addressed the effect of shape of monodispersed particles on apparent, poured and tap densities. They ultimately showed that the Hausner ratio decreases as the particles approach a spherical shape. The role of humidity on the apparent densities ratios, like the Hausner ratio, is apparently not clear so far, with contradictory data. Geldart & Wong (1984) observed that the Hausner ratio is slightly affected by the relative environmental humidity (RH), while data of Harnby *et al.* (1987) for glass spheres clearly indicate a strong effect for values of RH higher the 60%.

Santomaso, A.C., Lazzaro P., Canu, P. Powder flowability and density ratios: the impact of granule packing (2003) *Chemical Engineering Science,* 58 (13), pp. 2857-2874.
DOI:10.1016/S0009-2509(03)00137-4

3. Materials

In all the experiments aimed at characterize the flowability of density measurements several materials have been considered. They are listed in Table 1, together with basic properties such as intrinsic density and synthetic PSD information. Note that quite a broad range of sizes, intrinsic densities and chemical nature are involved. Iron particles are produced by Pometon SpA, and identified by code N20 and N60 (220 and 825 μm). Sands are mainly quartz, from local rivers. TAED is N,N,N',N'-tetraacetylendiamine in granular form, received by Caffaro SpA. Cellulose is type PH102 from FMR inc., barley is a commercial food product (Star SpA) in the form of roasted, soluble powders

PSD has been determined by sieving and then by image analysis of each fraction. Cohesive powders (i.e. cellulose, soluble barley, and lactose) are difficult to measure by image analysis, because of the aggregative nature and the presence of fines, so their PSDs have been determined by sieving only. Unfortunately, more than half of lactose particles falls below 37 μm, which is the smallest size of our set of sieves, so that its average diameter can not be consistently calculated. We will refer to the 'size' of the particles by the average diameter d_p (first column in Table 1).

The role of the restitution coefficient and of the particles shape has not been systematically investigated although it is expected to affect the results and must be eventually considered for a correlation. As recalled by Hayakawa & Hong (1997) the restitution coefficient plays a role in the energy dissipation of excited granular bed. Accordingly, some sort of influence in the packing dynamics should be expected.

4. Experimental methods

Experiments performed were mostly apparent density measurements, carried out with both standardized (or traditional) procedures, and new methods. These were essentially modifications of the former ones, aiming at reaching a higher reproducibility, and reliability thus. Results from our modified methods were surprising, since they directly impact the quantification of flowability. At the same time, static repose angle measurements were also carried out on the same materials, with the purpose of cross validating the conclusions on the flowability.

In the following we describe the methods with some detail, since we strongly believe that apparently obvious details can make a lot of difference in the results. Simple modifications to the standard procedure eventually resulted in measurements that consistently relate a wide spectrum of materials.

4.1. Apparent densities

As mentioned in the Introduction, there are several definitions of apparent density. We measured the *poured density* according to the International Standard ISO 3923-1 (equivalent to ASTM B 417 and EN 23923-1), frequently called funnel method. We built an apparatus along these Standards (Fig. 2a), that can also vary the distance between hopper and cup, from the prescribed 2.5 cm up to 1 m. Increasing the falling height is instrumental to our investigation, as described later. Since the measurements are very sensitive to small perturbations of the air flow around the falling powders as the hopper is elevated, we shielded the region between hopper and cup by means of a thin cylindrical surface, coaxial with the hopper and cup (Fig. 2b). Reproducibility was greatly enhanced with the shield. A test with TAED powders (440 μm) showed that the variance among 10 replicated measurements is always smaller with the shield, for any falling height. When pouring from 40 and 50 cm, the variance decreases by more than one order of magnitude when shielding is used. In the following we shall call *shielded* density the measure obtained by pouring the powders from

more than 2.5 cm, using the shield, and *poured* density the one at precisely 2.5 cm, without shield, as prescribed by ISO 3923-1 standard.

For all of the powders, both free-flowing and cohesive ones, we used the same hopper, with 60° aperture and a discharging nozzle of $5_0^{+0.2}$ mm diameter, a cylindrical collecting cup of volume 25±0.05 cm^3 and an internal diameter of 30±1 mm. Free flowing powders discharge uniformly and regularly from such a hopper, while cohesive materials require manual stirring in the hopper with a metallic wire, to remove them from the walls and make them flow through the outlet. The material surmounting the filled cup has been removed as carefully as possible, to avoid any compaction of the powders in the cup. Weighting has been performed with an accuracy of ±0.05 g and the final value taken as the average of 5 samples (i.e. 5 tests).

A second method has been developed, inspired by the Hosokawa Powder Characteristics Tester (Svarovsky, 1987; Harnby *et al.*, 1987; Abdullah & Geldart, 1999) and the standards ISO 3923-3 and BS EN 725-8. All of them suggest to help feeding poorly flowing powders by means of vibrating hoppers or making the powder to pass through a vibrating sieve. The procedure that we developed (Fig. 3) is partially modified with respect to the standards mentioned, since it allows varying the height of the hopper from 5 cm up to 1 m. Moreover, a special procedure for cohesive powders has been developed. Free-flowing granular material is fed by the hopper through a static sieve, at a distance of 1.5-2 cm from the discharging orifice (fig. 3a). The sieve serves the scope of dispersing as much as possible the particles flow after the orifice, making the granular material to rain down uniformly. The sieve mesh must be large enough to prevent the formation of arches on its holes. We experimentally determined this threshold for free-flowing powders to be 5-6 times the average particles diameter. Such a limit is also mentioned in the silos discharge literature and is connected with the minimum thickness of the shear zone (Nedderman & Laohakul, 1980; Santomaso, 2001).

Cohesive powders are more difficult to disperse. Consequently, we used a feeding cylinder of 4 cm inner diameter directly on the sieve (Fig. 3b), accurately filled to avoid compaction. Discharge is stimulated by translating the cylinder back and forth on the sieve, always in contact with it. A controlled flux of powders was then obtained. Apparent densities determined with both these procedures, based on the flow through a sieve, will be called *dispersed* in the following. Note that in this case shielding of the falling powder is not required since the results were found to be almost independent from environmental disturbances (except for cellulose). In addition, we chose a collecting cup of 25 cm^3 according to the Standard ISO 3923 and differently from the Hosokawa Powder Tester (which suggest 100 cm^3). Although a larger cup can reduce the wall effects (Scott, 1960; Zou & Yu, 1995) and the error due to surface leveling off, we preferred the smaller volume because of the large number of test to be performed, each one asking for a different sample of powder (as from the Standards). This procedure leads to a dense packing, as discussed in the following.

A third method to measure bulk density is based on the Copley apparatus to hit a powder, which is also the object of the International Standard ISO 3953 (ASTM B 527-93 or EN 23953). Again, we changed the indication of the Standards by replacing the graduated container with the same 25 cm^3 cup plus an extension (Fig. 4a) that double its volume. A graduated cup is not practical since reading is difficult after tapping, as already observed by Abdullah & Geldart (1999). The extended cup is filled through the funnel and then tapped with a manually rotated camshaft (Fig. 4b), applying a predetermined number N of strokes, at an approximate rate of 200 strokes/min. The extension is then

removed, powder leveled off as in the case of poured density and weighted the filled cup. In order to observe the effect of N, the extension can be remounted and, by the addition of more powder, repeat the whole sequence, applying the desired number N' of extra strokes. Typical sequences have been 100, 200, 400, 800, 1200 strokes, sometimes tapping until the desired final number of strokes, without intermediate measurements. The apparent density obtained with such a device will be called *tap density*, according to the classical definition, and aims at quantifying a dense packing condition.

Summarizing, several procedures have been devised to measure apparent densities, each one resulting in possibly different values, and were given different names. A synthetic picture is given in Fig. 7 to help orienting in the following.

4.2. Repose angle

Our goal is a revision of the density ratios in order to predict the flowability of granular materials. Eventually, some sort of validation must be envisaged. We chose the static repose angle to compare our flowability ranking based on modified density ratios. There are other flowability indexes but the static repose angle is expected to be the most insensitive to the initial powder compaction. The drained repose angle is meaningful only for non-cohesive granular material and is significantly influenced by the initial compaction degree (Svarovsky, 1987).

Slide angle and correlated ones are not uniquely determined, as demonstrated by Pouliquen & Renaut (1997) and Santomaso & Canu (2001). Such angles strongly depend on the nature of the surface on which the granular material flows (Augenstein & Hogg, 1978), and also on the initial thickness of the flowing layer.

Static repose angle has been measured with two different procedures, for free-flowing and cohesive powders, respectively. Free-flowing granular materials are the subject of ASTM C 1444 standard, developed for free-flowing mold powders. We used the same hopper as Fig. 2, with a discharging orifice 5 mm wide, instead of 6.4-9.7 mm (0.25-0.38 in.) prescribed, and a height of 40 mm instead of 38.1 mm (1.5 in.) of the standard (Fig. 8a). Powder is poured on the plane through the hopper, on a paper sheet with concentric graduated circles coaxial with the hopper's orifice, according to BS 4140 (1967) or ISO 902 standards for aluminum oxide powders. The diameter of the base D_A is taken as the average of 4 diameters. The repose angle is given by a simple geometrical construction as

$$\alpha_r = \tan^{-1}\left[\frac{2h}{(D_A - d)}\right] \qquad (2)$$

where d is the diameter of the orifice and h the height of the cone of powder. Measuring the repose angle with the procedure above is straightforward, for any non-cohesive powder, including barley.

With such a procedure lactose yields repose angles unusually low for this material. The reason appears to be the formation of aggregates in the hopper itself, of a size comparable with the discharging orifice. The aggregates tend to arrange in a cone the angle of which is much lower than expected for lactose powders. In order to obtain a measure of the angle for aggregating powders consistent with that of free-flowing materials, single particles must be made to fall on the slope of the cone. That means destroying the aggregates. We did that by means of a static sieve (200 μm), in the apparatus of Fig. 8b, similarly to the technique used to determine the dispersed density (Fig. 3b). We measured repose angles for lactose of 73°, much higher than 39° initially obtained. Note that the device shown in Fig. 8b does not discharge the material from an almost point source, so we decided

to keep the size of the base fixed, by allowing the powder to run off the edge of the collecting cup. Observe that such a modification implies a different mechanism of particle flow and packing. In the standard procedure, the height of the cone is predetermined and the base is allowed to enlarge; in our procedure the size of the base is constrained to remain fixed and the height is increasing. Consequently, the standard procedure works well for granular materials that can easily flow also on small slopes (significant horizontal translation component), while our procedure is suitable for materials that can stand steep slopes, were the particle flow is much more vertical. However, the height of the sieve above the cup determines some variability of the results, indicating that the momentum of falling particles can affect the shape of the growing cone. Eventually, we suggest the following procedure to measure the repose angle of cohesive powders. We select 3 sizes for the collecting cup (4.4, 2.1 e 0.75 cm) and performed several tests to identify the proper falling height such that the final cone tip is as close as possible (not more than 1 mm) to the sieve. In this condition 3 measurements were taken, for each cup. The angle chosen to be representative of the given material is the average of the 9 measurements. We believe that the effect of the size of the base is not significant by itself, but it reflects a different falling height, the real parameter that affects the measurements. The final kinetic energy (approximately proportional to the falling height) determines the slope of the building cone. Consequently, the results obtained with the smaller cup are expected to be more representative, since a lower height is required. We definitely recommend some investigation effort in this area, to eventually develop a consistent procedure. In the meantime, we believe that the average among several cup sizes contributes to smooth out the disturbances due to excess kinetic energy.

4.3. Volumetric solid fraction

In order to understand and mechanistically explain the differences in apparent density measured with several packing techniques, we developed a procedure to directly observe the volumetric solid fraction and its spatial distribution. We used a 'freezing' technique that we previously optimized to study mixing patterns (Santomaso et. al, 2002). We investigated only the 1000-1180 μm fraction of white, granular TAED, where the particles are easier to observe individually. Powder has been poured according to the two distinct procedures that result in the definition of *poured* and *dispersed* density, described above (i.e. pouring freely and through a static sieve, respectively). The hopper discharged from a height of 12 cm into a 6 cm diameter cup made of cardboard, internally lined with a vinylic glue film to make it paraffin-tight and suitable for subsequent slicing. The cup is filled for approximately 5 cm. To solidify the final bed, fused paraffin is percolated through. Paraffin was black colored to enhance the contrast with white particles. Additional details on the technique can be found in the mentioned work (Santomaso et. al, 2002) and by analogy also in Wightman *et al.* (1996). A similar technique to investigate packing efficiency was already used by Montillet & Le Coq (2001). They used it to study the shape effect on packing and the role of containing walls to orient non-spherical particles (actually plastics cylinders). We applied the freezing technique to observe the final structure of the beds of granular materials obtained with two different filling procedures. With this respect, the percolation of a high density fluid (melted paraffin) must not modify the initial structure of the bed. Ascertain this point is not so trivial. We indirectly assumed that there was no modification since the results semi-quantitatively confirm the expectations on the different packing mechanisms, as explained later.

Sliced surfaces have been analyzed with the MatLab Image Toolbox functions. Surfaces are scanned at 300 dpi, resulting in 775x775 pixels images, with a linear resolution of approximately 12 pixels/mm. The image is converted to black-and-white to discriminate particles from the background (the void between them). Surface solid fraction can be determined as the ratio of white to black pixels. Radial distribution can be evidenced by splitting the calculation on several (we used 350) concentric rings. Volumetric fraction can be correlated to surface fraction through the following approximated equation:

$$v_{3D} = \frac{4}{3\pi^{1/2}} v_{2D}^{3/2} \qquad (3)$$

suggested by Campbell & Brennen (1985), among others. However, eq. (3) was derived for monodispersed spheres, regularly arranged in a lattice. Eq. (3) underestimates the volumetric solid fraction in the case of polydispersed granules, randomly packed. It is more conservative then to apply the simplest

$$v_{3D} = v_{2D}^{3/2} \qquad (4)$$

assuming a locally isotropic spatial distribution of granules.

5. Comparison among packing techniques.

The main objective of the study is a search for a procedure to obtain a more reliable measure of density representative of a dense random packing. The initial hypothesis, later confirmed, was that the poor reliability of the Hausner's ratio to correlate powder flowability is due to the ambiguity and variability of the higher density (tap) measure. Following such hypothesis, we compared the results of different density measurement procedures susceptible to produce a dense packing. The dense packing condition is traditionally assumed to be the one resulting from tapping, as described in Sec. 4.1. In this technique several strokes are applied until a minimum volume is achieved. Our apparatus (Fig. 4) behaves quite reproducibly. Fig. 5 shows a typical result of these measurements, for a lactose powder. Note that the initial density depends on the reproducibility of the initial filling of the cup, but eventually the same asymptotic value is reached anyway. Accordingly, the procedure for the initial filling does not require much attention. Manual tapping through the cam was found to yield more reproducible results than manually hitting the cup or by making it to fall from a given height (Svarovsky, 1987).

Density obtained by pouring can increase with the falling height and can be alternative techniques to obtain a dense packing. Shielded and dispersed density values have been taken as the average of 5 independent replicas. We chose 5 points (like Abdullah & Geldart, 1999) instead of the 3 suggested by some Standards (e.g. EN 23923-1 and 2, and EN 23953) because we sought for a more precise measurement for further comparisons. The number of tests (5) for each sample and condition chosen was determined with a fairly long sequence of 15 measurements, shown in Fig. 6. Besides observing that the maximum experimental error never exceeds 1% and is mostly within 0.5%, it is apparent that the progressive averages stabilize fairly rapidly. Based on these data, the optimum number of replicas appears to be 7. We thought that 5 is a good compromise between accuracy, time and material required. A further check was performed on lactose and summarized in Table 2 in terms of decrease of variance with increasing numbers of replicas. Observe the significant increase of reproducibility from 3 to 5 runs, particularly for measurements at the lower falling height.

Both shielded and dispersed density can be affected by the falling height. Fig. 9 shows a typical behavior (iron powders), where the increase of both densities is clearly seen, up to an asymptotic

value. Interestingly, they can become higher (4.4% in the case of Fig. 9) than tap density, determined according to the Standards. This means that a suitable feeding procedure can lead to higher packing than insisting in hitting from the outside an inappropriately filled vessel. Observe also from Fig. 9 that the dispersed density grows higher than the shielded one, though both apparently point to the same asymptote. The general features highlighted above and shown in Fig. 9 for iron are common to all free-flowing powders. The same sequence of measurements reported in Fig. 9 has been repeated for all the powders of Tab. 1. Asymptotic results together with other density measurements for all the materials considered are summarized in Tab. 3. The actual behavior of each powder at increasing height is discussed in the following, in order to evidence the role of specific material feature.

5.1. Effect of average particle size and true density

Different granule sizes were available for most materials. Iron and ballottini were received at two different granules sizes and have a good roundness. Other granular materials were originally significantly polydispersed. In principle, size fractions could be obtained by sieving. We did it for sand and TAED, isolating fairly narrow size classes. However, we concentrated on iron and ballottini to investigate the size effect since sand and TAED add the effects of shape, surface roughness and of a residual dispersion in their respective size classes.

Fig. 10 shows the results of varying the falling height for iron with a size (220 μm) smaller than in Fig. 9. Once again, we observe that the dispersed density is higher than tap one, even for the lowest falling height. At the same time, we see that the packing achievable by pouring from a point source (the orifice) is not significantly affected by the falling height, also isolating the environmental disturbances (shielded density) that are larger for smaller particles. The asymptotic convergence of dispersed and shielded densities for the smaller iron particles cannot be confirmed by the data of Fig. 10.

Results for glass ballottini, also available in two size classes, are shown in Fig. 11. Dispersed densities are again higher than tap ones (not shown in the figure for clarity, but reported in Tab. 3) and stabilize with height, although for smaller particles growth is not constant. As for the smaller iron granules, both classes of ballottini result in a shielded density that barely increases with falling height. It must be observed that the smallest particles (107 μm) behave quite irregularly for low falling height and a clearly distinguishable growth of dispersed density begins only above a certain height.

At this point we can simply conclude that a small particle size and a lower intrinsic density both result in a divergence between the dispersed and shielded density measurements, the latter barely stabilizing on an asymptotic value.

The variation with height of the solid volumetric fraction, ν, provides some additional indication. This fraction can be directly evaluated from the ratio between a bulk density and the intrinsic density. When the dispersed density is used as bulk density, quite a regular increase of packing with height is obtained, shown in Fig. 12 (above). This is not the case when the poured (shielded) density is used (data not shown). The smallest glass particles behave differently indicating that packing by gravity must compete with interparticle forces, that can become significant as the particle size decreases. 100 μm should not be such a small size to evidence large interparticle force effects, but consider that Ballottini 107 contains particles as small as tens of microns, where electrostatic effects can play a role.

Apparently, the dispersed density proved to be a very suitable procedure to obtain the highest packing of granular materials. The ultimate value can vary sensibly with the particle size distribution and particularly with the presence of fines. These are present in all the materials tested, as confirmed by the data in Table 1, but the relative incidence is larger for the smaller particles. A larger amount of fines in the smaller (220 μm) iron particles (see Tab. 1) explains the slightly higher packing achieved with respect to the larger iron particles (825 μm). Fines can also be impurities and that is reflected by the discrepancies in the intrinsic densities reported in Table 1, for the same type of material. Trying to remove fines from iron 220 results in a significant increase of measured true density, clearly pointing at the value measured for iron 825. Figure 12 (above) also shows a different increase of packing at the lowest falling heights, particularly clear comparing iron and ballottini of similar (220-230 μm) size. This is a consequence of the inappropriate comparison of different materials based on the same falling height. Better agreement in the transient part of Fig. 12 (above) is obtained plotting the data with respect to $z\rho$, as in Fig. 12 (below). This product is equivalent to a specific potential energy, at the given height. It is apparent that size and material differences tend to vanish in the transient part. Discrepancies remain in the asymptotic solid volumetric fraction and for the smaller glass particles, as discussed above. Potential energy can be seen as the maximum energy available to drive the dissipative packing process. The actual energy available when the particles impact onto the bed is given by the kinetic energy, which depends upon the particle velocity at the impact. A model of a single spherical particle fall in quiescent air has been developed to predict the particle acceleration due to gravity, possibly reaching the terminal falling velocity. According to the model, many of our granular materials do not reach the steady terminal velocity in our experiments, even falling from 1 m. The evolution of the solid fraction in terms of velocity at the impact can be useful to understand the packing mechanism. However, monodispersed particles must be used to clearly discuss this point, in conjunction with a particle fall model that should also account for departures from single particle condition. This will be the subject of a future work. So far, Fig. 12 allows concluding that the dispersed density suggested in this work appears to better describe the packing process, unifying the behavior of granular materials of different size and density.

5.2. Effect of particle size and shape distributions

TAED and sand particles shapes are quite different from spherical, as observed by microscopy (roundness ϕ=0.70 and ϕ=0.74 respectively). In addition, each size fraction was obtained by sieving a rather broad PSD of the material as received. TAED is also a fairly brittle material that tends to produce fines when sheared. Accordingly, these granular materials are suitable to get some insight into the complex role of particle size and shape distributions. Measurements taken with TAED are reported in Fig. 13. The purpose of such measurements was not a thorough investigation on the role of both size and shape distribution, but simply aim at confirming that 'real' granular materials behave like better defined and selected ones. Specifically, Fig. 13 shows that i) bulk densities determined by pouring increase with falling height, ii) the dispersed technique always reaches a stable asymptote, iii) such asymptotic value is always higher than tap density (see Tab. 3). At the same time, the uncontrolled possible presence of fines in each size class causes a strange correlation of the results with the average particle size, with the largest particles having an intermediate dispersed density, and the smallest an intermediate shielded density.

5.3. Cohesive powders

All the free-flowing powders behave like data of Fig. 9, with some disturbances for smaller size particles, as shown in Fig. 11. Eventually, the dispersed density can always be uniquely determined and turns out to be the highest packing achievable without compaction. Cohesive powders are more difficult to define, first, and then characterize. Roasted barley powders for food use is an example of an apparently free-flowing granular material that we classified among cohesive ones, as justified later. Its measurement of densities is shown in Fig. 14. Many features are different with respect to free-flowing powders. The most evident is that dispersed density does not grow higher than tapped one (9% below, in this case), while always reaching an asymptotic value. This is not the case of shielded density which does not stabilize with height and usually becomes higher than dispersed one, above some height (i.e. profiles cross at some height). Note that data for shielded density are lacking at higher elevation, since the flow of these powder looses coherence and becomes dispersed. Very similar behavior is shown by lactose powders, Fig. 15. Here the tapped density is not shown for clarity, since it is much higher than the asymptotic dispersed density. We believe that both aspects, tap and protected densities higher than dispersed one, are caused by the nature of these materials that make them difficult to pack, but much easier to compact. While it is intuitive the higher propensity to compact the granular material of the procedure to obtain tapped density, it is less for the shielded density. However, shielded density is obtained by pouring from a point source, differently from the dispersed one. This allows the powder to convey a larger momentum per unit surface to the collecting cup, facilitating some compaction to take place. We will discuss this interpretation further in the following discussion.

6. Discussion on the density measurements

In this section we try to formulate a mechanistic explanation of the observations reported above, aiming at concluding that the procedure resulting in what we called the dispersed density has several advantages in terms of reproducibility and physical consistency.

The results for free-flowing granular materials reported above clearly indicate that the dispersed density is always the highest obtainable, sometimes at very low falling height. We believe this can be explained by looking closely at the mechanism by which powders fall in the cup to fill it. Standard procedures to obtain the poured density (but also our attempt to protect the falling material by shielding) feed the granular material to the collecting cup from a concentrated source, which is the hopper's orifice. The granules tend to fall on the same point in the cup, dissipating most of the momentum vertically, on the underlying material already accumulated. Because the growing cone in the cup rapidly exceeds the repose angle, additional material flows along the slope, after the initial vertical impact on the top. The residual momentum used in this translation is much lower than the original one, due to the falling height, mostly dissipated vertically on top of the cone. Accordingly, the resulting structure of the bed of powder in the cup is intuitively uneven. Powders close to the axis of the cup are more densely packed, and possibly partially compacted, with respect to the surrounding ones. Peripheral areas in the cup accumulate powders with a much looser packing, with a structure approaching the aerated condition, resulting from the accumulation of granules by rolling down the slope of the growing cone. The procedure developed for the dispersed density tries to work around this limitation, changing the way powders are fed to the cup. In this case a regularly distributed flow of powders feed the cup, so that each granule dissipates all is momentum in the point where it hits the material already accumulated in the cup, or in close proximity. The granules in

Santomaso, A.C., Lazzaro P., Canu, P. Powder flowability and density ratios: the impact of granule packing (2003) *Chemical Engineering Science,* 58 (13), pp. 2857-2874.
DOI:10.1016/S0009-2509(03)00137-4

the surface layer retain some mobility as far as the pressure of the further material above them has not grown enough. Consequently, surface granules can rearrange towards a minimum of potential energy (i.e. lower position that implies a higher packing) under the uniform drive given by the momentum of the falling granules. The kinetic energy of the incoming granules is totally used to overcome local friction resistances among granules, achieving the minimum energy configuration. Accordingly, very closely packed layers build up in the cup, where the filling does not occur through a cone anymore. Such a mechanism was suggested also by Pouliquen *et al.* (1997), who obtained a regular, high density packing of spheres by leading them to a minimum of potential energy through horizontal vibrations involving a few surface layers only.

Interestingly, the procedure leading to dispersed density distributes the same mass flow rate of granular material over a larger surface, which eventually implies a slower falling velocity for the particles. It has been experimentally proved by Ogata *et al.* (2001) that the same solid flow rate leads to higher particle velocity if a denser, jet-like structure is realized. Accordingly, the velocity profile across the flow of particles falling on the cup can be schematically represented as in Fig. 16. The lower velocity at the borders is due to the larger dissipation of momentum in shearing the initially static air around the jet. In the central region the entrained air has a smaller velocity difference with respect to the falling particles and hence particle can acquire a higher velocity. Note that the width of the bell-shaped profile increases with flow path (i.e. falling height). Accordingly, when the material is poured from a point, at small distances slower particles reach the peripheral regions of the cup, while above a certain height the granules reach the cup with a rather flat velocity profile. This explains the convergence of the shielded and dispersed measurements at increasing height.

The most direct prove of the mechanism just explained would be the experimental observation of a radially varying porosity. We attempted to do this by the freezing, slicing and image analysis technique described above. The result of such a test with white TAED in black paraffin is shown in Fig. 17 as binary (B/W) images. It is immediately apparent that the density of particles after pouring from a point source (image on the left) is higher in the centre of the section, while is more uniform in the case of dispersed density (right). In addition, the ordered accumulation of particles at the border can be easily recognized. More quantitative information is given by the statistics of the number of white pixels in concentric rings, as explained in Sec. 4.3. Results for both sections of Fig. 17 are shown in Fig. 18. The general features are confirmed by the quantitative profiles also, with a clearly decreasing solid fraction towards the periphery of the cup in poured density technique. The highest density at the walls is also quantitatively confirmed by the solid fraction profiles. Taking the average of each profile one can calculate the surface fraction of solid. Again, the poured density results in a lower average, 0.562 vs. 0.607 of the dispersed one. Interestingly, surface solid fraction in the boundary ring, where the wall causes an ordered packing, shows that dispersion leads to higher packing here too (0.71 vs. 0.63). Surface solid fraction can be converted to volumetric solid fraction through eq. (4) and then to bulk density with the true density of the granular material used (1330 kg/m^3). Calculations for the averages give 560 and 628 kg/m^3, for poured and dispersed density, respectively. Such figures from image analysis are surprisingly close the results of Fig. 13 at z=0.1 m, i.e. 587 and 621 kg/m^3, gravimetrically obtained. We believe that the better agreement for dispersed density could be a demonstration that there is some swelling effect due to paraffin, which is negligible in a more uniform granular bed. However, we believe that the freezing technique to analyze solid fraction distributions must be more thoroughly validated in order to speculate in detail on its quantitative results.

Santomaso, A.C., Lazzaro P., Canu, P. Powder flowability and density ratios: the impact of granule packing (2003) *Chemical Engineering Science,* 58 (13), pp. 2857-2874.
DOI:10.1016/S0009-2509(03)00137-4

6.1. Revision of flowability indexes

The density measurements reported above and the discussion on the packing mechanism definitely suggest taking advantage of the procedure developed to consistently obtain dense packing without compaction, to revise flowability criteria based on density. Tap to dispersed density ratio in Tab. 3 already shows that materials are divided between two classes. One has the dispersed density higher than tap one and the other is the contrary. Intuitively free-flowing powders like sand, iron and ballottini belong to the first class, while the second category contains powders typically known as cohesive, like lactose.

In addition, we attempt to extend the application of such criteria seamlessly to granular material classified as cohesive. In a sense, a flowability criteria can be seen also as cohesiveness criteria, considering that cohesion is considered the predisposition of granules to stick one to each other, a process that limit particles movements and hence overall granular flow.

In view of a quantification of flowability, the ratio known with the name of Hausner already introduced above is a good choice. It properly compares the packed and dilated condition for the same powder. This is relevant for flowability since it has been observed since a long time ago (Reynolds, 1885) that granular material must dilate to start flowing. However, the Hausner's ratio which uses as numerator the tap density defined above is known to be severely dependent on the operator and hence critical in its use in the industrial practice. Having done the thorough experimental investigation reported above, on the achievement and measurement of dense packing, we conclude that the limitations of the Hausner's ratio are connected with the measurement of tap density. We already mentioned that such a measure is only partially standardized and even in those cases where indications exist, ambiguities remain. Powders can be tapped manually, while filling the cup or when the cup is full. Tapping can be obtained by dropping the cup from a given height or through some kind of machinery with different frequency, amplitude or intensity of vibrations or strokes. Moreover, the total numbers of strokes are conventionally given round number by Standards or Pharmacopeias (typically 500 or 1250) with the indication that the minimum volume must be achieved. However, the final result may overlook specific features of the powder that were apparent in the packing process, if the different number of strokes to achieve the final goal is not relevant, nor recorded. It is not unusual that the same powder with a different degree of moisture can be forced, by changing the total number of strokes, to achieve the same final tap density, while it is dramatically evident the different flowing behavior. Perhaps the most critical objection to the tap density procedures is the uncontrolled packing obtainable. Not only its uniformity in space is not guaranteed by the procedures, but such packing can also easily become a compaction, i.e. forcing the particle to modify their shapes to reach a higher filling.

Additional evidences about the weakness of the Hausner's ratio arose from our experiments. We systematically measured the repose angle of all the materials used, according to the procedures detailed in Section 4.2 above. Fig. 19 shows the values of *HR* for several free-flowing powders (repose angle smaller that approx. 45°). The figure demonstrates that the repose angle differentiates the granular materials considered, while *HR* is at best insensitive, if not randomly correlated. *HR* remains close to 1.06 while the repose angle varies by almost 20°. It is quite surprising that *HR* cannot account for such significant differences in flowing behavior. Such a low resolution of the *HR* within the free-flowing powders was already observed, as clear from Tab. 4 (De Jong *et al.* 1999). Both Flow Factor and *HR* apparently do not distinguish the last three different degrees of flowability, while the repose angle does report quite significant variations among these categories.

Santomaso, A.C., Lazzaro P., Canu, P. Powder flowability and density ratios: the impact of granule packing (2003) *Chemical Engineering Science,* 58 (13), pp. 2857-2874.
DOI:10.1016/S0009-2509(03)00137-4

Similar conclusions can be drawn for the results reported in Fig. 20, taken for monohydrate lactose samples, kept at different environmental humidity for at least 24h. Again, HR remains approximately constant at 1.65 while the repose angle varies by some 15°. This confirms that *HR* is a measure independent of the moisture content, as already reported (Geldart & Wong, 1984), but unfortunately it also substantiates the conclusion that *HR* is quite a scarce flowability index. Lactose powders left at different environmental humidity demonstrated very different flowing behavior, indeed.

Plotting all the above data of *HR* together with those of cellulose and barley at different *RH* we obtain Fig. 21. Barley and cellulose have been introduced only now since their flow behaviour is more ambiguous, varying from free-flowing to cohesive. Fig. 21 shows that HR does not report a continuous variation between free-flowing and cohesive behaviour, apparently tracking the flowability variations by steps, distinguishing classes instead of degrees of flowability.

The *HR* of barley is surprisingly sensitive to the environmental humidity, whereas the repose angle is less. This special behaviour can be explained with the nature of this powder, which is intended to be dissolved in some liquid (milk or water) for its use. Barley solubility adds to the hygroscopicity also shown by lactose and cellulose, dramatically changing particle properties, that become sticky eventually leading to irreversible aggregation (i.e. compaction).

According to the critical evaluation of HR reported above and the improvements in measuring a dense packing density with the procedure leading to the dispersed density, we attempted to formulate a novel flowability index. We retain the idea behind the Hausner's ratio, of comparing a loose to a dense packing condition, but simply replaced the tap with the dispersed density as a measure of the latter state. Fig. 22 shows the correlation between such a revised ratio and the repose angle. It is quite evident a more continuous variation with the material flow properties as measured by the repose angle. The new density ratio is almost linear when plotted vs. the square root of the tangent of the repose angle, as shown in Fig. 23.

From Fig. 21 and 22 (or better, Fig. 23) we can conclude that density ratios can effectively measure the flowability, but the original formulation (*HR*) that uses the tap density results in loss of sensitivity for quite wide classes of materials. Such a limitation of *HR* disappears if a different technique is used to obtain a dense packing.

It was clear from earlier experiments that the procedure leading to tapped density was causing some compaction in addition to packing with powders like lactose, barley and cellulose. Emptying the cup was sometimes difficult with these materials due to the formation of a solid plug. That was not the case in poured density measurements, even with the easiest material to compact (lactose), nor with the dispersed density. These observations led us to believe that *HR* is not actually comparing two states of the powders that reflect the same physical mechanism of packing. Procedure to obtain tapped density can seriously cause a significant compaction with certain granular material, while the poured density can hardly determine some compaction to take place, and also the dispersed density was obtained with a procedure that prevents any detectable compaction. As a result, the revised density ratio compares two configurations of different degree of packing, hence expression of the same physical mechanism, at two limiting conditions. Accordingly, we suggest to call the ratio of dispersed to poured density Packing Ratio (*PR*).

Not only *HR* includes some contribution to the density due to compaction, but apparently the *HR* ratio is more sensitive to the compaction than the packing degree. Powders reported in Fig. 19 are undoubtedly different in terms of flowability, but all share the same negligible propensity to compact,

and *HR* does not vary among them. At the other extreme, monohydrated lactose with a repose angle above 60° can change its flowability with the moisture content, but it always remains a granular material very easy to compact; again, *HR* does not distinguish the different degrees of flowability (Fig. 20), but it definitely reports a different value with respect to the difficult-to-compact material of Fig. 19, as clear from Fig. 21. Barley changes dramatically its compaction with moisture, due to its soluble nature, and *HR* varies accordingly, while cellulose compaction is not significantly affected by moisture and hence the corresponding values of *HR.* The sensitivity of *HR* to compaction introduces in the analysis additional particle properties, such as its resistance to deformation. Such properties are connected with the flow process, but the *HR* does not clearly account for them quantitatively.
Compaction hinders granular flow so *HR* is correlated to flowability anyway, but less directly, perhaps because tapped density is not meant to be a measure of compaction, notwithstanding the fact that its procedure causes some compaction to arise. The influence of compaction on flowability mixes with that of packing, so a proper analysis should isolate the two physical mechanisms. We believe that the *PR*, thanks to the dispersed density, successfully isolates the pure packing effect. A further confirmation can be the regular variation with the repose angle. In the repose angle measurement procedure, we eventually achieve locally, on the slope, a packing condition not confined by any wall, as a result of interparticle rearrangements similar to those quantified by the *PR*. The ratio of *PR* to *HR* should be a measure of the role of compaction, according to the discussion above. It turns out to be simply the ratio of tapped to dispersed densities, already reported in Tab. 3:

$$\frac{PR}{HR} = \frac{\rho_{dispersed}}{\rho_{tap}},$$

Its variation with the repose angle is reported in Fig. 24. It clearly allows to discriminate between granular materials that simply pack with those that accompany some compaction to the packing process. Powders of the first type concentrate in the left quadrant above, while those affected by compaction cluster in the lower right quadrant. Interestingly, the regions are naturally divided by a ratio of 1, at an abscissa of 1 in the transformation of the repose angle (square root of its tangent) that makes its correlation with *PR* linear. In absolute terms, this means that powders that simply pack have a dispersed density always higher than tapped one and repose angles below 45°, and the contrary for powders that are susceptible to compaction. This provides also a criteria to classify powders between cohesive and free-flowing.

7. Conclusions

This work started with some simple observations on the dramatic influence of experimental procedures on the measurement of apparent density. We eventually suggested a reproducible procedure to achieve a dense random packing condition without inducing powder compaction. We called *dispersed density* the property measured along this procedure and in some cases it can be higher than tap density. We characterized and discussed the structure of the resulting granular bed in terms of particle distribution in space and rearrangement mechanism.
The observations above directly impact the quantification of flowability by means of apparent density ratios, such as Hausner's one. Based on the dispersed density we suggest a novel flowability index, that we called *packing ratio (PR)*. We adopted the repose angle as an independent scale of flowability to compare these ratios with. The *PR* turns out to be more continuously sensitive to flowability variations, also in those cases where *HR* does not distinguish any significant difference among granular materials. Moreover, *PR* apparently can describe free-flowing and cohesive powders

consistently. Note that the lack of standard procedures to measure the repose angle for cohesive granular material called us to develop a specific technique. We critically tested it on a few cohesive materials, but independent and wider validation is required in order to develop a unique technique for both cohesive and free-flowing powders.
PR shows a linear correlation with the square root of the repose angle, up to quite high values (80°). We believe that a connection with the microstructure of the packing could explain such a relation, but we did not attempt to investigate.
Some variables have not properly investigated and should be included in further developments. These include the particle shape, particularly when very different from spherical, like prismatic crystals or needle-like powders, and the restitution coefficient, very likely to play a role in granular flow. In addition, powders flowability does not depends purely on packing degree, as described by *PR*, but compaction can also affect the flow properties. The latter is partially included in the *HR,* the information of which is different than *PR.* A proper combination of the two indexes may increase our ability to characterize and predict the flow of granular materials, by means of more reliable and grounded procedures than the actual ones.

8. References

Abdullah, E. C. & Geldart, D. (1999) The use of bulk density measurement as flowability indicators. *Powder Technology* 102, 151-165.
American Society for Testing and Materials (1989) Standard test method for apparent density of non-free-flowing metal. ASTM B 417 - 89 (reapproved 1995).
American Society for Testing and Materials (1993) Standard test method for determination of tap density of metallic powders and compounds. ASTM B 527 - 93 (reapproved 1997).
American Society for Testing and Materials (1994) Standard test method for apparent density of powders using the Arnold meter. ASTM B 703 - 94 (reapproved 1999).
American Society for Testing and Materials (1996), Standard test method for apparent density, bulk factor and pourability of plastic materials. ASTM D 1895 - 96.
American Society for Testing and Materials (1997) Standard test method for flow rate of metal powders. ASTM B 213 - 97.
American Society for Testing and Materials (1998) Standard test method for apparent density of metal powders and compounds using the Scott volumeter. ASTM B 329 - 98.
American Society for Testing and Materials (1999) Standard test method for apparent density of free-flowing metal powders using the Hall flowmeter funnel. ASTM B 212 - 99.
American Society for Testing and Materials (1999) Standard test method for measuring the angle of repose of free-flowing mold powders. ASTM C 1444 - 99.
Augenstein, D.A. & Hogg, R. (1978) An experimental study of the flow of dry powders over inclined surfaces. *Powder Technology* 19, 205-215.
Bates, L. *User guide to segregation*, BMHB, Bucks, 1997
Bernal, J. D. & J. Mason (1960) Co-ordination of randomly packed spheres. *Nature* 188, 910-911.
British Standard (1986) Methods test for aluminum oxide Part9: Measurement of the angle of repose. Replaces BS Addendum n.1 (1970) to BS 4140 (1967).

Santomaso, A.C., Lazzaro P., Canu, P. Powder flowability and density ratios: the impact of granule packing (2003) *Chemical Engineering Science,* 58 (13), pp. 2857-2874.
DOI:10.1016/S0009-2509(03)00137-4

Campbell, C.S. & Brennen, C.E. (1985) Computer simulation of granular shear flows. *Journal of Fluids Mechanic* 151, 167-188.

De Jong, J. A. H., Hoffmann, A. C. & Finkers, H. J. (1999) Properly determine powder flowability to maximize plant output. *Chemical Engineering Progress*, April 1999, 25,34.

Edwards, S.F. & Grinev, D.V. (1998) Statistical mechanics of vibration-induced compaction of powders. *Physical Review E* 58, 4758-4762.

Edwards, S.F. & Oakeshott, R.B.S. (1989) Theory of powders. *Physica A* 157, 1080-1090.

European Committee for Standardization (1993), Metallic powders - Determination of apparent density - Part 1: Funnel method. EN 23923 - 1 (ISO 3923 - 1: 1979).

European Committee for Standardization (1993), Metallic powders - Determination of apparent density - Part 2: Scott volumeter method. EN 23923 - 2 (ISO 3923 - 2: 1981).

European Committee for Standardization (1993), Metallic powders - Determination of tap density. EN 23953 (ISO 3953: 1985).

European Committee for Standardization (1997), Advanced technical ceramics - Methods of test for ceramic powders - Part 8: Determination of tapped bulk density. EN 725 - 8.

European Pharmacopoeia – 2nd edition - Part II - Seventeenth fascicule (1993), printed and published by Maisonneuve S.A., Saint-Ruffine, France.

Geldart, D. & Wong, C.Y. (1984) Fluidization of powders showing degrees of cohesiveness-I. Bed expansion. *Chemical Engineering Science* 39, 1481-1488.

Harnby N., Hawkins, A.E. & Vandame D. (1987) The use of bulk density determination as a mean of typifying the flow characteristics of loosely compacted powders under conditions of variable relative humidity. *Chemical Engineering Science* 42, 879-888.

Hayakawa, H & Hong, D. C. (1997) Thermodynamic theory of weakly excited granular systems. *Physical Review Letters* 78, 2764-2767.

International Organization for Standardization (1976) Aluminium oxide primarily used for the production of alluminum - Measurement of the angle of repose. First edition. ISO 902 (1976).

Knight, J.B., Fandrich, C.G., Lau, C.N., Jaeger, H.M. & Nagel, S.R. (1995) Density relaxation in a vibrated granular material. *Physical Review E* 51, 3957-3963.

Lesaffre, C., Mineau, V., Picart, D. & Van Damme, H. (2000) Densification under vibration of a saturated granular packing. *Acad. Sci. Paris*, t. 1, Séries IV, 647-653.

Linz, S.J (1996) Phenomenological modeling of the compaction dynamics of shaken granular systems. *Physical Review E* 54, 2925.

Montillet, A. & Le Coq, L. (2001) Characteristics of fixed beds packed with anisotropic particles - Use of image analysis. *Powder Technology* 121, 138-148.

Nedderman, R.M. & Laohakul, C. (1980) The thickness of the shear zone of flowing granular materials. *Powder Technology* 25, 91-100.

Nowak, E.R., Knight, J.B., Piovinelli, M.L., Jaeger,H.M. & Nagel, S.R. (1997) Reversibility and irreversibility in the packing of vibrated granular material. *Powder Technology* 94, 79-83.

Ogata, K., Funatsu, K. & Tomita, Y. (2001) Experimental investigation of a free falling powder jet and the air entrainment. *Powder Technology* 115, 90-95.

Ouchiyama, N. and Tanaka, T. (1989) Predicting the densest packing of ternary and quaternary mixtures of solids particles. *Ind. Eng. Chem. Res.* 28, 1530-1536.

Pouliquen & Renaut (1996) Onset of granular flows on an inclined rough bed: dilatancy effect. *Journal de Physique II* 6, 923-935.

Pouliquen, O., Nicolas, M. & Weidman, P.D. (1997) Crystallization of non-Brownian spheres under horizontal shaking. *Physical Review Letters* 79, 3640-3643.
Reynolds, O. (1885) On the dilatancy of media composed of rigid particles in contact with experimental illustrations. *Philosophical Magazine* 20, 469-481.
Santomaso, A. & Canu P. (2001) Transition to movement in granular chute flows. *Chemical Engineering Science* 56, 3563-3573.
Santomaso, A. (2001) Bachelor Thesis, Univ. of Padua.
Santomaso, A., Olivi, M. & Canu P. (2002) Mixing of granular matters in a rotating cylinder: rolling regime patterns. To be submitted to *Chemical Engineering Science*.
Schwedes, J. (1996) Measurement of flow properties of bulk solids. *Powder Technology* 88, 285-290.
Scott, G. D. (1960) Packing of equal spheres. *Nature* 188, 908-909.
Suzuki, M., Sato, H., Hasegawa, M. & Hirota, M. (2001) 53-57 Effect of size distribution on tapping properties of fine powder. *Powder Technology* 118, 53-57.
Svarovsky, L. *Powder testing guide: methods of measuring the physical properties of bulk powders*, published on behalf of BMHB by Elsevier Applied Science, London and New York., 1987.
Tsirel, S.V. (1997) Methods of granular and fragmented material packing density calculation. *International Journal of Rock Mechanics and Mining Science* 34, 263-273
Wightman, C., Muzzio, F.J. & Wilder, J. (1996) A quantitative image analysis method for characterizing mixtures of granular materials. *Powder Technology* 89, pp. 165-176.
Wong, A. C. -Y. (2000) Characterisation of the flowability of glass beads by bulk densities ratio. *Chemical Engineering Science* 55, 3855-3859.
Yu, A. B., Bridgwater, J. & Burbidge (1997) On the modelling of the packing of fine particles. *Powder Technology* 92, pp. 185-194.
Yu, A.B. and Standish N. (1991) Estimation of the porosity of particle mixture by linear-mixture packing model. *Ind. Eng. Chem. Res.* 30, 1372-1385.
Zou, R. P. & Yu, A. B. (1995) The packing of spheres in a cylindrical container: the thickness effect. *Chemical Engineering Science* 50, 1504-1507.
Zou, R. P. & Yu, A. B. (1996) Evaluation of the packing characteristics of mono-sized non-spherical particles. *Powder Technology* 88, 71-79.

List of symbols and acronyms

d_p	(average) particle diameter [μm]
d	diameter of the hopper orifice [m]
D_A	diameter of the base of the cone [m]
B	Parameter in eq. (1)
FF	Flow Factor (De Jong et al. 1999)
h	height of the cone of powder [m]
HR	Hausner's ratio
m_p	Particle mass [kg]
N	Number of strokes
RH	Relative (environmental) humidity [%]
PSD	Particle size distribution

Santomaso, A.C., Lazzaro P., Canu, P. Powder flowability and density ratios: the impact of granule packing (2003) *Chemical Engineering Science,* 58 (13), pp. 2857-2874.
DOI:10.1016/S0009-2509(03)00137-4

z	Falling height [m]
α_r	Static repose angle [°]
$\Delta\rho$	Parameter in eq. (1)
Γ	Vibration intensity (= acceleration/g)
v, v_{3D}	Volumetric fraction of solid
v_{2D}	Surface fraction of solid
ρ	Density (generic) [kg/m^3]
ρ_O	Parameter in eq. (1)
ρ_s	Density of the solid (intrinsic)
τ	Parameter in eq. (1)
ϕ	Roundness = 4π Area/Perimeter^2

FIGURES

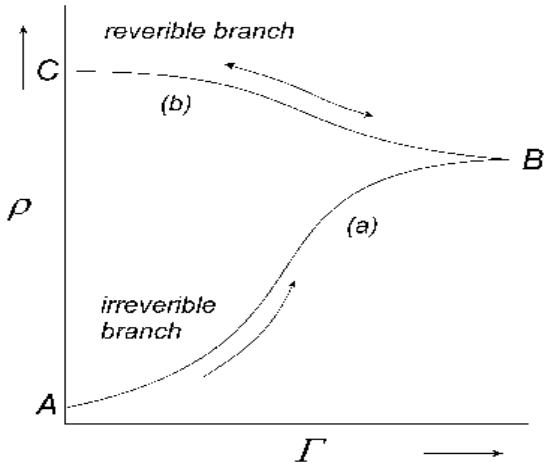

Figure 1 Variation of the apparent density with vibration intensity Γ. (adapted from Novak *et al.*, 1997)**.**

Santomaso, A.C., Lazzaro P., Canu, P. Powder flowability and density ratios: the impact of granule packing (2003) *Chemical Engineering Science,* 58 (13), pp. 2857-2874.
DOI:10.1016/S0009-2509(03)00137-4

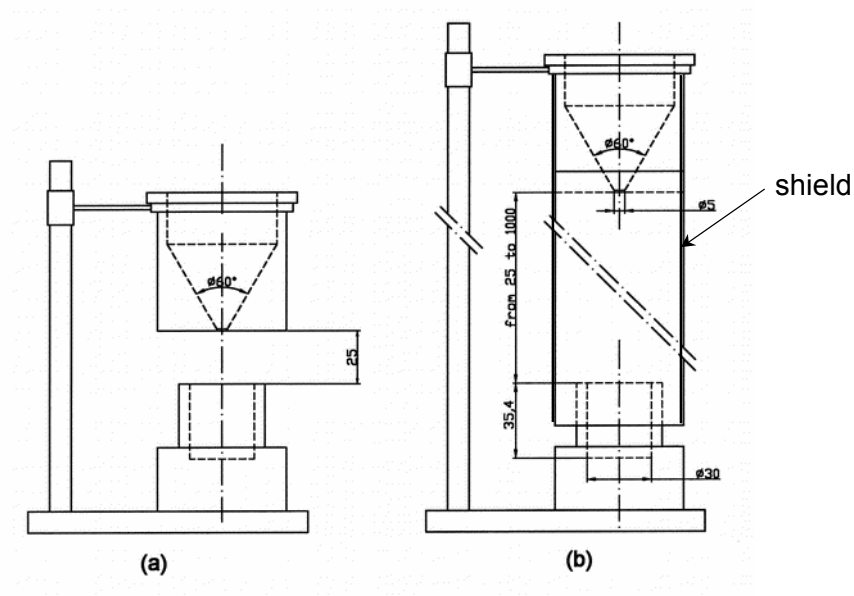

Figure 2 Experimental apparatuses for determination of apparent density: poured (a) and shielded (b). All dimensions in mm.

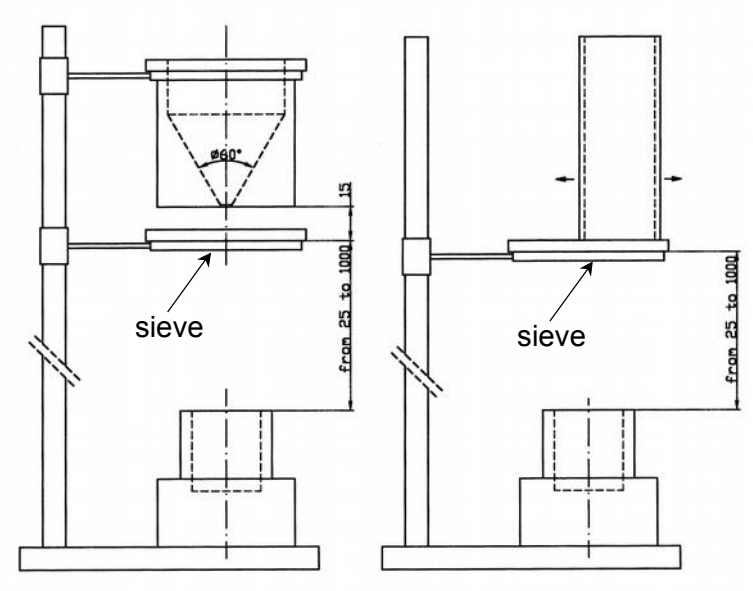

Figure 3 Experimental apparatuses for determination of apparent density. Measurement of dispersed density. Free-flowing (a) and cohesive (b) powders. All dimensions in mm.

Santomaso, A.C., Lazzaro P., Canu, P. Powder flowability and density ratios: the impact of granule packing (2003) *Chemical Engineering Science,* 58 (13), pp. 2857-2874.
DOI:10.1016/S0009-2509(03)00137-4

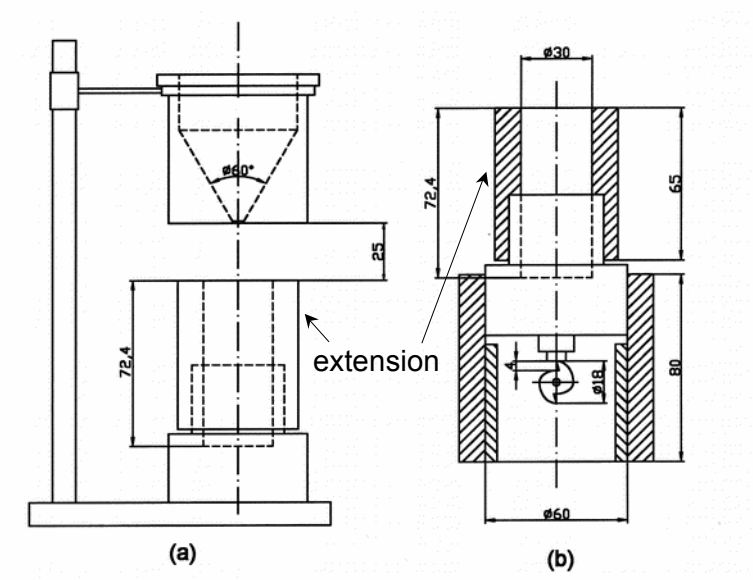

Figure 4 Experimental apparatus for determination of tap density. Funnel, cup and extension (a) and tapping machinery (b). All dimensions in mm.

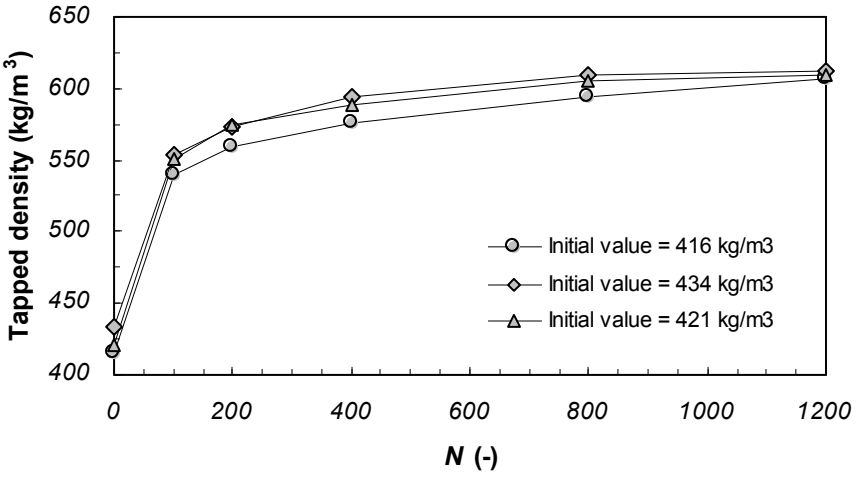

Figure 5 Typical increase of tap density with the number of strokes, starting from different initial filling arrangements. Monohydrate lactose at 45% RH.

Santomaso, A.C., Lazzaro P., Canu, P. Powder flowability and density ratios: the impact of granule packing (2003) *Chemical Engineering Science,* 58 (13), pp. 2857-2874.
DOI:10.1016/S0009-2509(03)00137-4

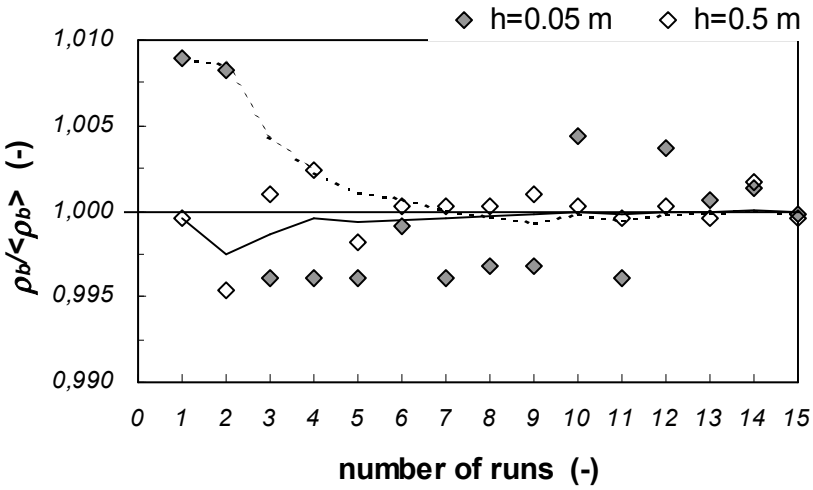

Figure 6 Ratio of bulk (poured) density measurements in 15 independent runs and the average over all the 15 tests (symbols). Progressive average (lines). TAED 733 μm freely falling from 0.05 or 0.50 m.

Figure 7 Classification and nomenclature for different densities defined and measured in this work. Note that both shielded and dispersed density varies with falling height, so that the result can be a loose or dense packing condition. For this reason the shielded density was put between the two categories, while the dispersed density was assigned to the dense packing category because we always consider its higher, asymptotic value.

Santomaso, A.C., Lazzaro P., Canu, P. Powder flowability and density ratios: the impact of granule packing (2003) *Chemical Engineering Science,* 58 (13), pp. 2857-2874.
DOI:10.1016/S0009-2509(03)00137-4

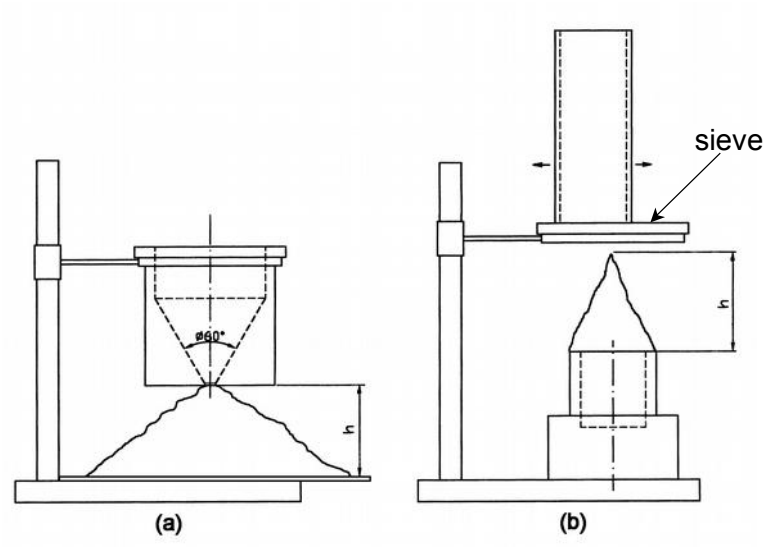

Figure 8 Experimental apparatuses for determination of static repose angle. Free-flowing (a) and cohesive (b) powders.

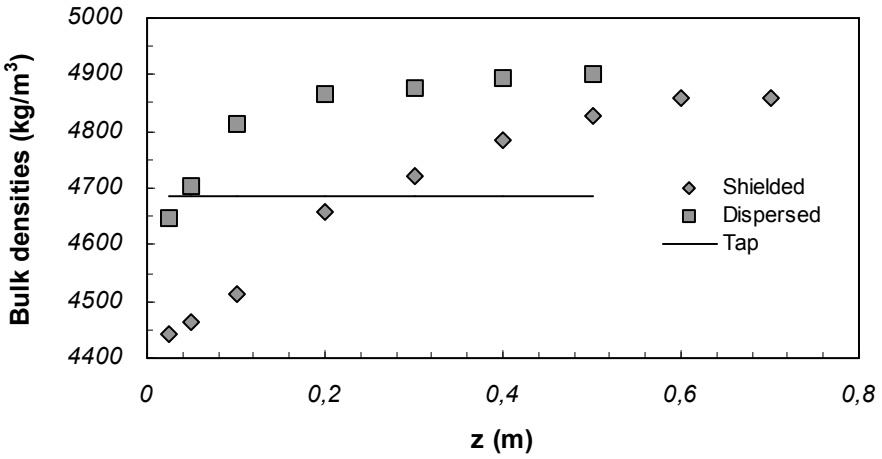

Figure 9 Effect of falling height on shielded and dispersed density, and comparison with tap density (1000 strokes). Iron 825 μm.

Santomaso, A.C., Lazzaro P., Canu, P. Powder flowability and density ratios: the impact of granule packing (2003) *Chemical Engineering Science,* 58 (13), pp. 2857-2874.
DOI:10.1016/S0009-2509(03)00137-4

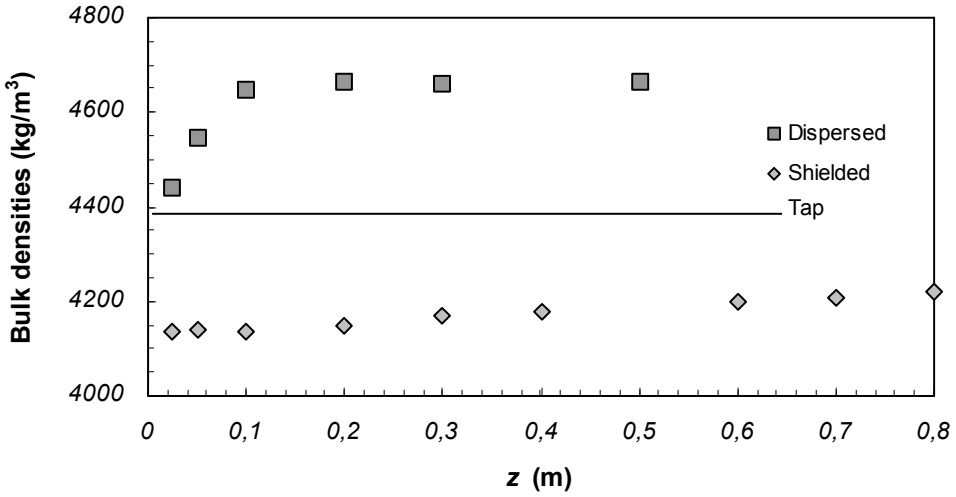

Figure 10 Effect of falling height on shielded and dispersed density, and comparison with tap density (line). Iron 220 μm.

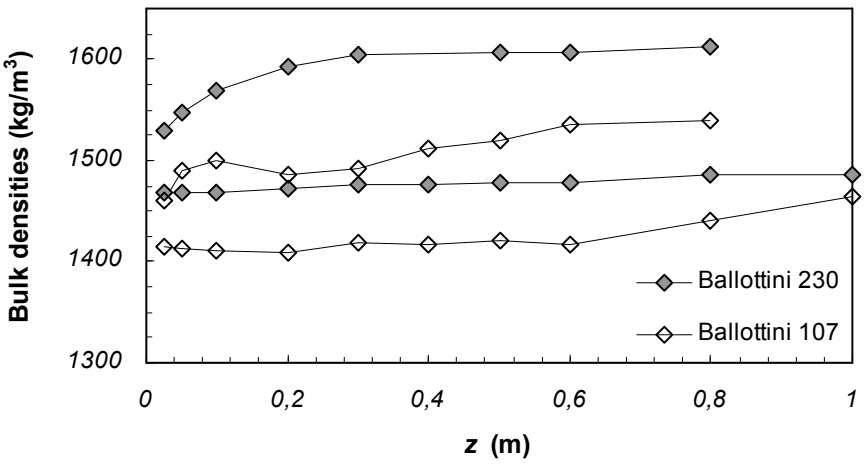

Figure 11 Effect of particle size and falling height on shielded (dashed lines) and dispersed (solid lines) density. Ballottini 230 and 107 μm.

Santomaso, A.C., Lazzaro P., Canu, P. Powder flowability and density ratios: the impact of granule packing (2003) *Chemical Engineering Science,* 58 (13), pp. 2857-2874.
DOI:10.1016/S0009-2509(03)00137-4

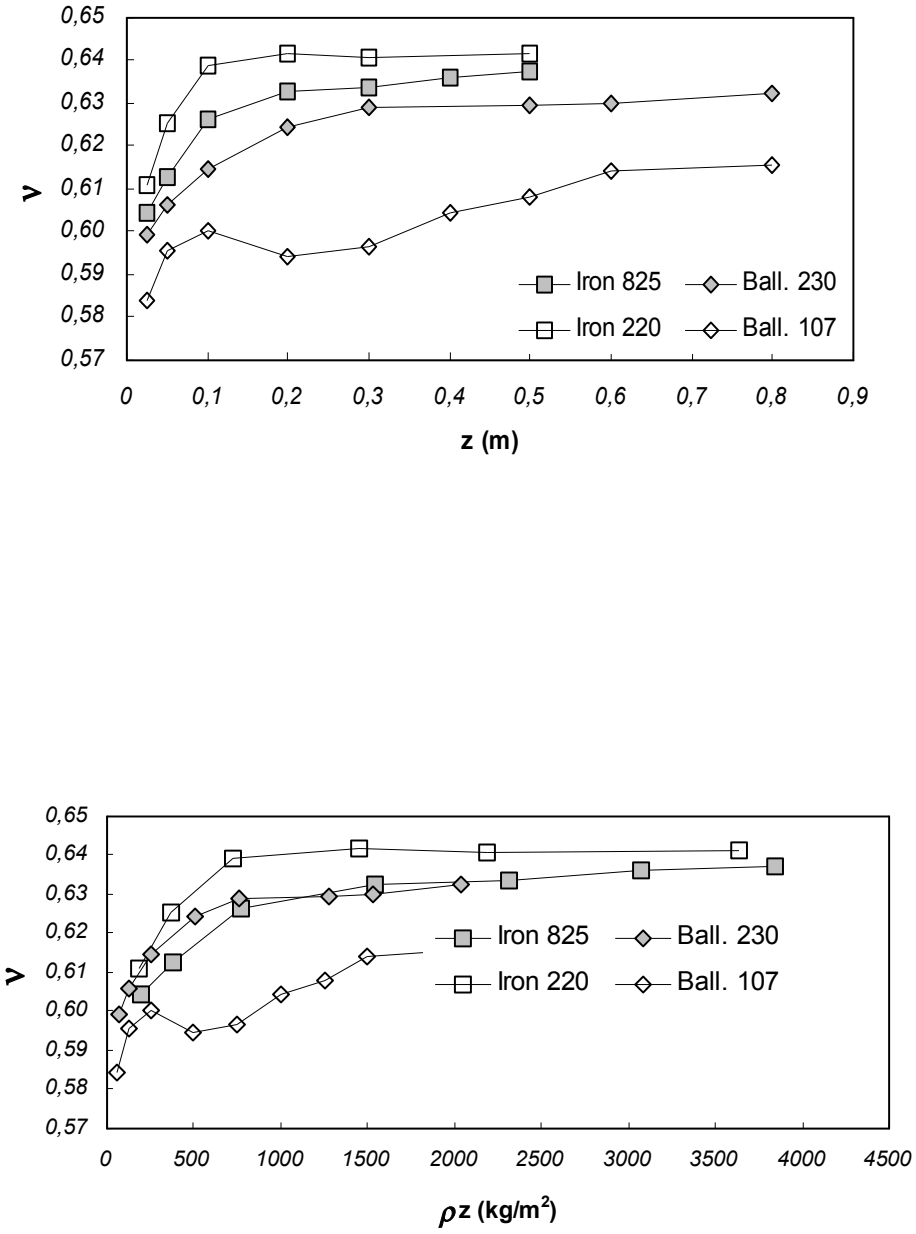

Figure 12 Variation of the solid volumetric fraction, based on dispersed density, with height (top) and specific potential energy (bottom). Iron 825 and 230 μm and ballottini 230 μm and 107 μm.

Santomaso, A.C., Lazzaro P., Canu, P. Powder flowability and density ratios: the impact of granule packing (2003) *Chemical Engineering Science,* 58 (13), pp. 2857-2874.
DOI:10.1016/S0009-2509(03)00137-4

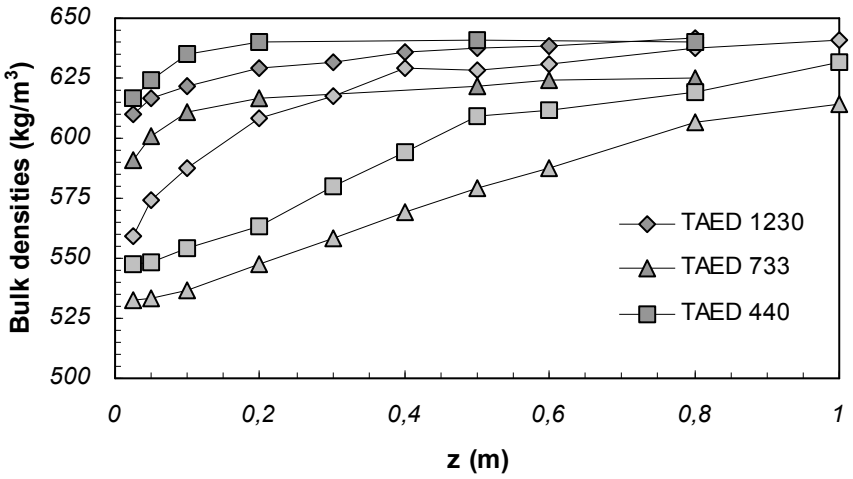

Figure 13 Effect of falling height on shielded (dashed lines) and dispersed (solid lines) density for 3 size classes (440 μm, 733 μm, and 1230 μm) of TAED.

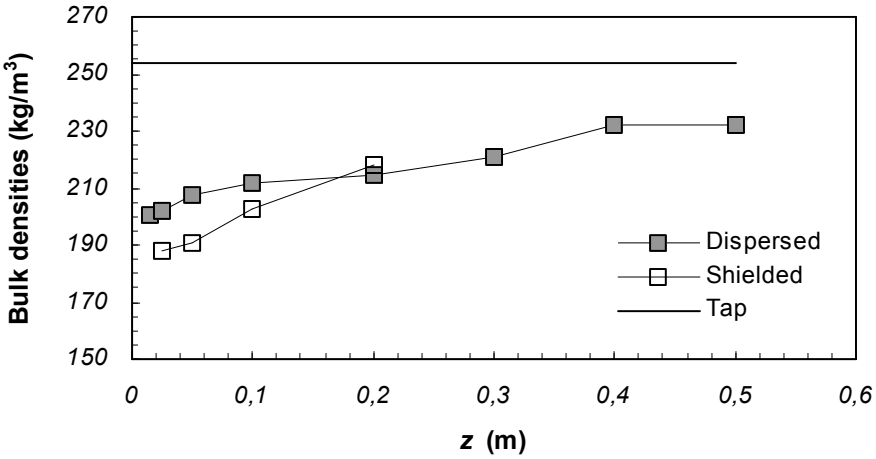

Figure 14 Effect of falling height on shielded and dispersed density, and comparison with tap density (1000 strokes). Barley 165 μm, at 40% RH.

Santomaso, A.C., Lazzaro P., Canu, P. Powder flowability and density ratios: the impact of granule packing (2003) *Chemical Engineering Science,* 58 (13), pp. 2857-2874.
DOI:10.1016/S0009-2509(03)00137-4

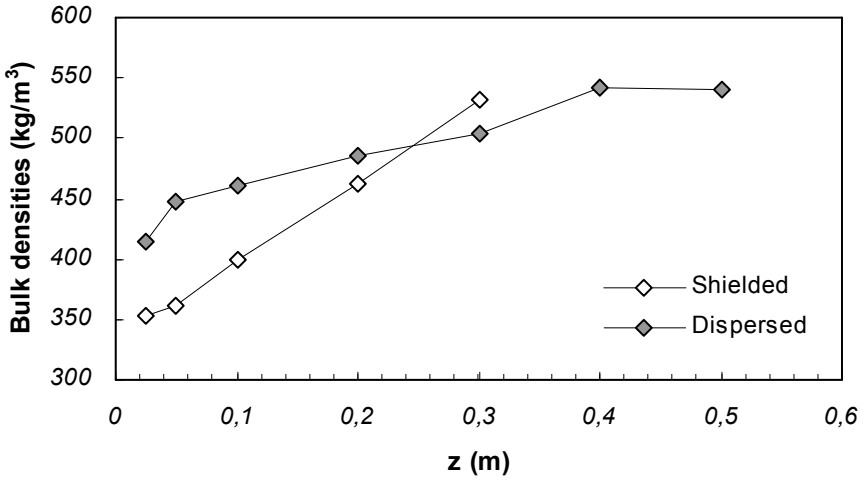

Figure 15 Effect of falling height on shielded and dispersed density. Lactose, at 31% RH.

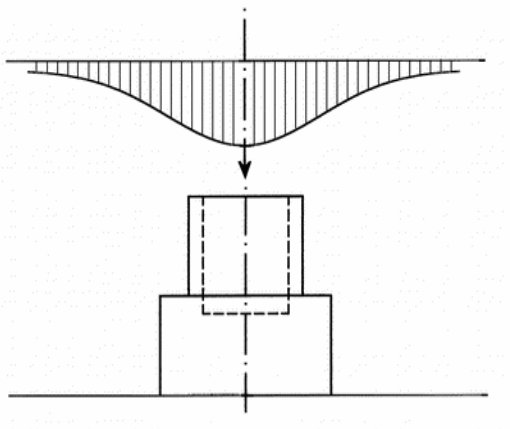

Figure 16 Schematic picture of the particle velocity profile (vertical component) across the flow of material falling on the cup.

Santomaso, A.C., Lazzaro P., Canu, P. Powder flowability and density ratios: the impact of granule packing (2003) *Chemical Engineering Science,* 58 (13), pp. 2857-2874.
DOI:10.1016/S0009-2509(03)00137-4

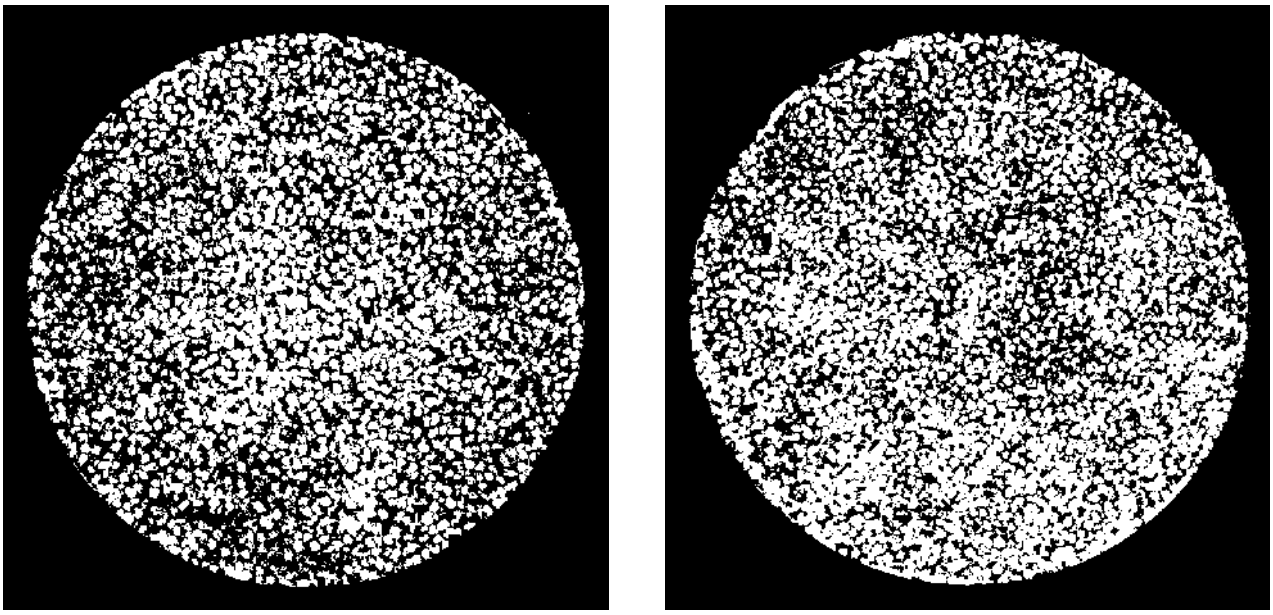

Figure 17 Sections (approx. 1cm from the bottom) of the powder accumulated in the cup by pouring simply from a funnel (left) or through a sieve (right), resulting in the shielded and dispersed density techniques, respectively. White TAED 1230 in black paraffin.

Santomaso, A.C., Lazzaro P., Canu, P. Powder flowability and density ratios: the impact of granule packing (2003) *Chemical Engineering Science,* 58 (13), pp. 2857-2874.
DOI:10.1016/S0009-2509(03)00137-4

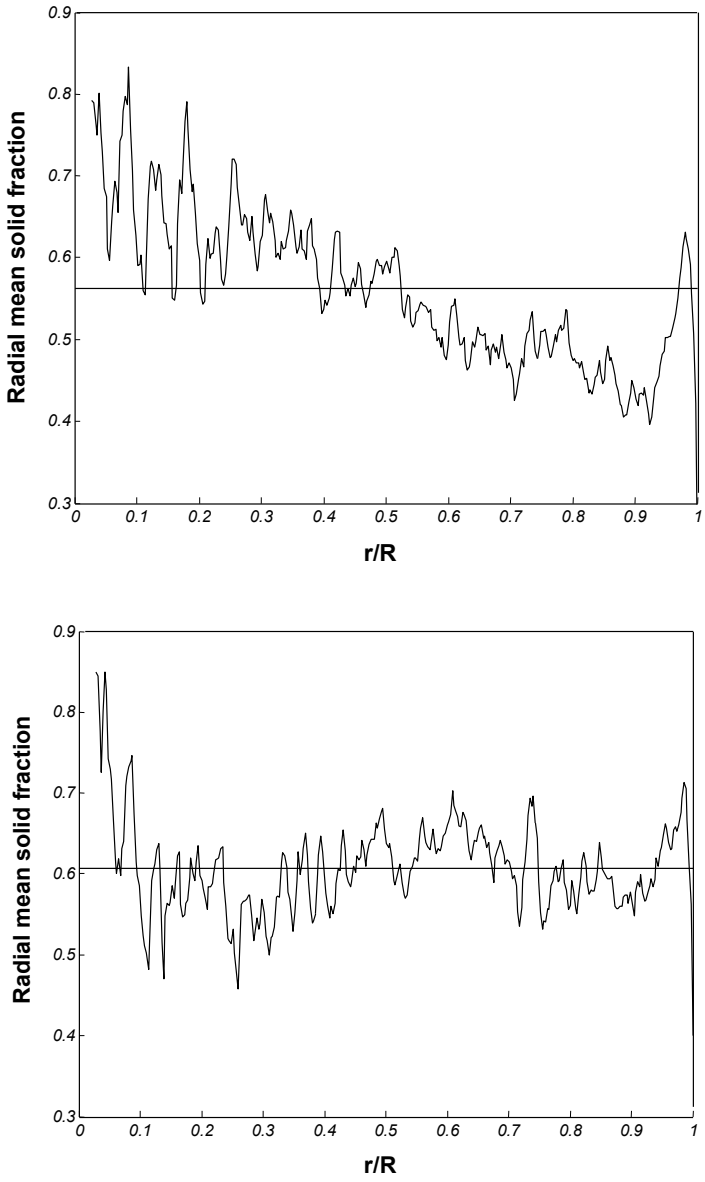

Figure 18 Radial distribution of solid (surface) fraction for shielded (top) and dispersed density (bottom), calculated from Fig. 17.

Santomaso, A.C., Lazzaro P., Canu, P. Powder flowability and density ratios: the impact of granule packing (2003) *Chemical Engineering Science,* 58 (13), pp. 2857-2874.
DOI:10.1016/S0009-2509(03)00137-4

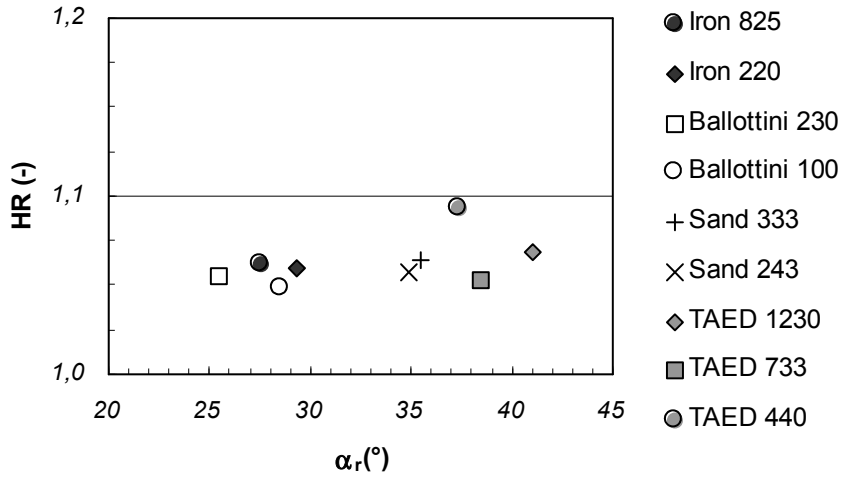

Figure 19 Hausner's ratio vs. repose angle. Free-flowing powders ($\alpha_r < 45°$).

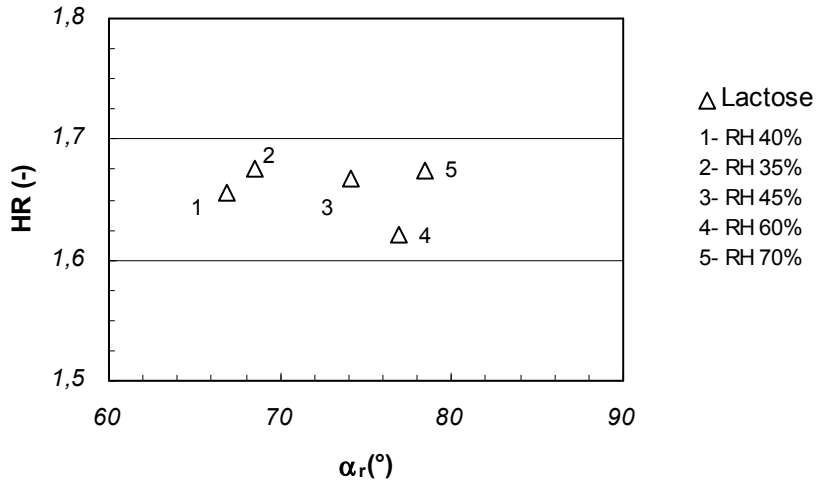

Figure 20 Hausner's ratio vs. repose angle. Lactose, after 24h at different environmental humidity.

Santomaso, A.C., Lazzaro P., Canu, P. Powder flowability and density ratios: the impact of granule packing (2003) *Chemical Engineering Science,* 58 (13), pp. 2857-2874.
DOI:10.1016/S0009-2509(03)00137-4

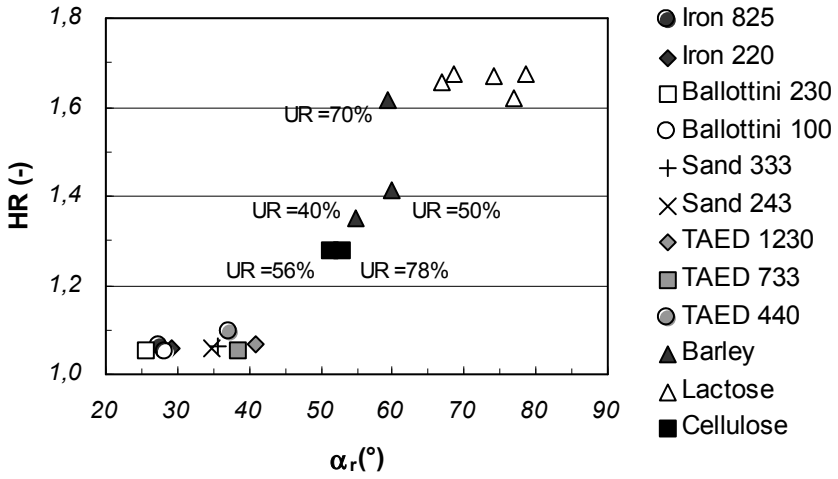

Figure 21 Hausner's ratio vs. repose angle. All the materials of Figs. 19 and 20, with the addition of barley and cellulose, both at different environmental humidity.

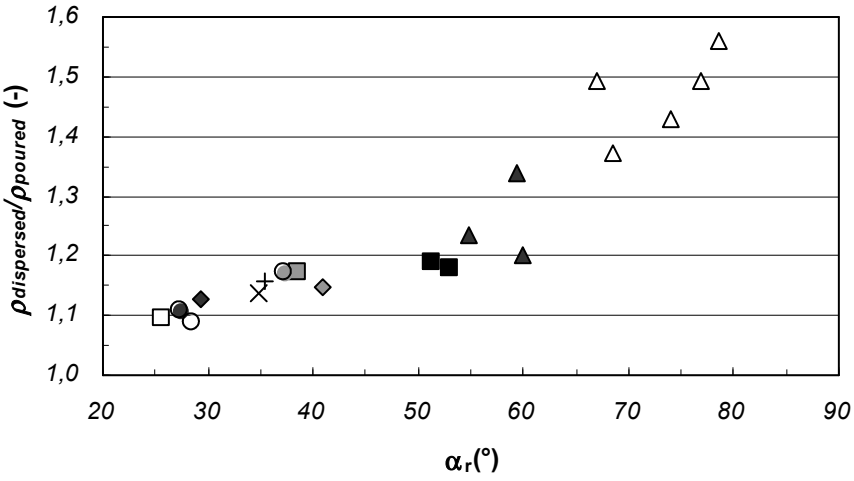

Figure 22 Ratio between dispersed and poured densities vs. repose angle. All the materials, possibly at different environmental humidity. Same symbols of Fig. 21.

Santomaso, A.C., Lazzaro P., Canu, P. Powder flowability and density ratios: the impact of granule packing (2003) *Chemical Engineering Science,* 58 (13), pp. 2857-2874.
DOI:10.1016/S0009-2509(03)00137-4

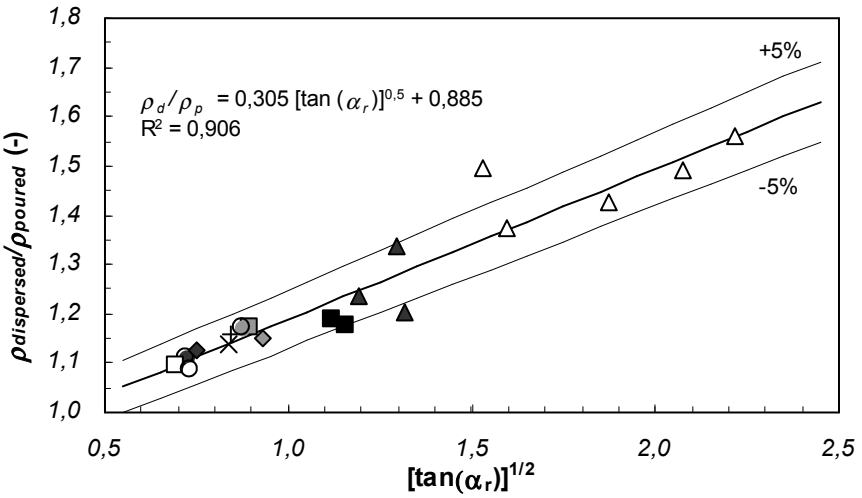

Figure 23 Ratio between dispersed and poured densities vs. repose angle (rescaled). Same symbols of Fig. 21. Linear interpolation (solid line) and ±5% range (dashed line).

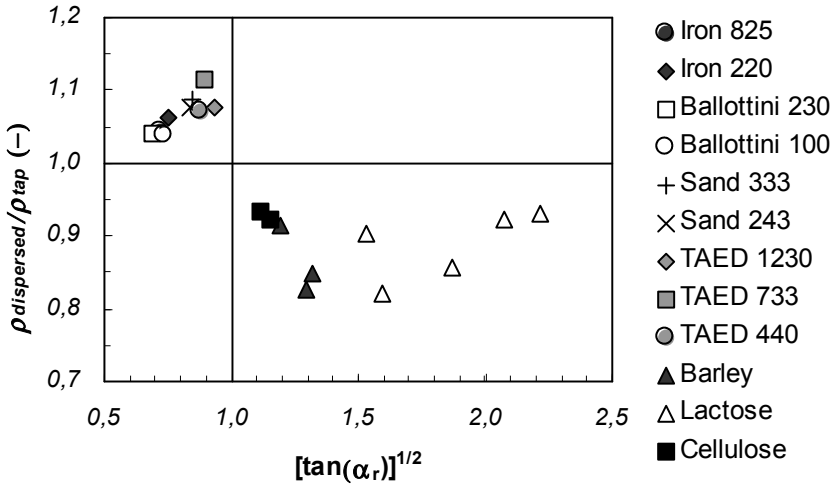

Figure 24 Classification of powders with respect to packing and compaction propensity. Same symbols of Fig. 21.

Santomaso, A.C., Lazzaro P., Canu, P. Powder flowability and density ratios: the impact of granule packing (2003) *Chemical Engineering Science,* 58 (13), pp. 2857-2874.
DOI:10.1016/S0009-2509(03)00137-4

TABLES

Table 1 Properties of the materials used in this study.

Material	d_p μm	$d_{p\,(10\%)}$ μm	$d_{p\,(50\%)}$ μm	$d_{p\,(90\%)}$ μm	ρ_s kg/m^3
Iron	825	735	800	915	7692
Iron	220	175	210	265	7270
Ballottini	230	185	225	275	2550
Ballottini	107	90	116	124	2500
Sand	333	290	350	375	2630
Sand	243	220	235	265	2630
TAED	1230	1090	1210	1370	1330
TAED	733	630	740	835	1330
TAED	440	380	450	500	1330
Cellulose	105	30	92	180	1430
Barley	165	105	160	225	825
Lactose	/	/	48	72	1530

Table 2 Decrease of variance of poured density measurements, with increasing numbers of replicas. In brackets the ratio with respect to s^2(15 runs). Monohydrated lactose.

	$s^2_{\,3\ runs}$	$s^2_{\,5\ runs}$	$s^2_{\,7\ runs}$	$s^2_{\,15\ runs}$
0.05 m	$2.263\ 10^{-5}$ (4.1)	$1.348 \cdot 10^{-5}$ (2.4)	$9.746 \cdot 10^{-6}$ (1.7)	$5.582 \cdot 10^{-6}$ (1)
0.5 m	$3.610 \cdot 10^{-6}$ (4.3)	$2.542 \cdot 10^{-6}$ (3)	$1.706 \cdot 10^{-6}$ (2)	$8.247 \cdot 10^{-7}$ (1)

Santomaso, A.C., Lazzaro P., Canu, P. Powder flowability and density ratios: the impact of granule packing (2003) *Chemical Engineering Science,* 58 (13), pp. 2857-2874.
DOI:10.1016/S0009-2509(03)00137-4

Table 3 Numerical results of the different densities and repose angle measured for all the materials considered. All densities in kg/m^3.

	Poured density	**Dispersed density**	**Tap density**	**True density**	**Dispersed/ Tap**	**Dispersed/ True**	**Repose angle (°)**
Iron 825	4413	4892	4685	7692	1.044	0.636	27.5
Iron 220	4137	4664	4385	7270	1.064	0.642	29.3
Ballottini 230	1468	1613	1548	2550	1.042	0.633	25.5
Ballottini 100	1416	1539	1484	2500	1.037	0.616	28.5
Sand 333	1442	1669	1535	2630	1.087	0.635	35.5
Sand 243	1414	1609	1495	2630	1.076	0.612	34.9
TAED 1230	559	642	597	1330	1.075	0.483	41.0
TAED 733	532	625	560	1330	1.116	0.470	38.5
TAED 440	547	640	598	1330	1.070	0.481	37.4
Cellulose (78% RH)	299	357	382	1440	0.935	0.248	51.2
Cellulose (56% RH)	305	360	390	1440	0.923	0.250	53.0
Barley (70% RH)	172	230	278	825	0.827	0.279	59.3
Barley (50% RH)	178	214	252	825	0.849	0.259	60.0
Barley (40% RH)	188	232	254	825	0.913	0.281	54.8
Lactose (70% RH)	350	546	586	1530	0.932	0.357	78.5
Lactose (60% RH)	353	527	572	1530	0.921	0.344	76.9
Lactose (45% RH)	367	524	612	1530	0.856	0.343	74.1
Lactose (40% RH)	358	535	593	1530	0.902	0.350	66.9
Lactose (35% RH)	367	504	615	1530	0.820	0.329	68.5

Santomaso, A.C., Lazzaro P., Canu, P. Powder flowability and density ratios: the impact of granule packing (2003) *Chemical Engineering Science,* 58 (13), pp. 2857-2874.
DOI:10.1016/S0009-2509(03)00137-4

Table 4 Classification of flowability through several Indexes (adapted from De Jong *et al.,* 1999).

	Flow Factor	***HR***	α_r
Non flowing	<2	>1.4	>60
Cohesive	2-4	>1.4	>60
Fairly free-flowing	4-10	1.25-1.4	45-60
Free-flowing	>10	1-1.25	30-45
Excellent flowing	>10	1-1.25	10-30
Aerated	>10	1-1.25	<10